

System identification and feedback control for directed-energy, metal-based additive manufacturing

D. M. Seltzer*, X. Wang§, A. R. Nassar†, J. L. Schiano*, E. W. Reutzel†,

*School of Electrical Engineering and Computer Science, § Department of Mechanical and Nuclear Engineering, †Applied Research Laboratory,
The Pennsylvania State University, University Park, PA 16802

Abstract

Additive manufacturing of metal parts is a complex process where many variables determine part quality. In addition to manipulated process variables, such as travel speed, feedstock flow pattern, and energy distribution, other exogenous inputs also determine part quality. For example, changing build geometry and a growing global temperature. In addition, there are random external disturbances such as spatter on a cover lens. Both manipulated process variables and exogenous inputs affect dimensional tolerance, microstructure, and other properties that determine the final part quality. Our long term aim is to improve part quality through real-time regulation of measurable process variables using vision-based feedback control. As a starting point, we present a process model that relates scanning speed and laser power to build height and melt pool width. These results demonstrate the necessity for using multi-input multi-output feedback control techniques and provide information for refining the frame rate and spectral sensitivity of the imaging system.

1. Introduction

Feedback control is essential for maintaining consistent part quality in metal-based additive manufacturing (AM) processes because of variations in build geometry and temperature [1]. Previous control designs represent the AM process as being either a single-input single-output (SISO) process [2-4], or more realistically, as a multi-input multi-output (MIMO) process [5-6]. Few studies explicitly state the reason for selecting the manipulated variable(s), and for those that did, the reasoning was qualitative rather than quantitative. What distinguishes this work from earlier studies, is that the MIMO feedback design is driven by the measured sensitivity of process variables to manipulated inputs, and, that the real-time camera measurements are verified using optical profilometer measurements following the deposition.

This work has three specific aims. The first is to use experimental measurements to identify a MIMO dynamic model that relates the scanning speed and laser power to the build height and melt pool width. The second aim is to quantify the sensitivity of each process output with respect to each process input. The third aim is use the measured sensitivities and identified model to design and simulate a MIMO control design for regulating melt pool width and build height.

Melt pool geometry is recorded in real-time using a monochrome camera and, for verification, post deposition using an optical profilometer. These measurements facilitate computation of sensitivity metrics and identification of dynamic models. The dynamic models are then used to evaluate feedback control designs using numerical simulations.

Two salient results emerge from this work. First, discrepancies between the optical profilometer and real-time camera measurements place a lower bound on the camera frame rate and indicate the importance of appropriately choosing the optical wavelengths at which images are acquired. Second, it is necessary to use a MIMO AM process model when designing feedback control systems so that all process outputs remain within desired ranges.

2. Experimental Setup

Additive manufacturing experiments use an Optomec LENS MR-7 laser-based, directed-energy-deposition system. The LENS system utilizes a 500 watt, Ytterbium-doped fiber laser (IPG YLR-500-SM). The working distance is 0.365 in, as measured from the substrate to four radially-symmetric powder delivery nozzles. Centered within the four powder nozzles is a center-purge nozzle through which argon flows coaxially onto the substrate.

A custom designed-and-built, sensor-mounting fixture surrounds the laser processing head. Mounted onto the fixture is a monochrome camera for viewing the melt pool. The optical axis of the camera is approximately 45° with respect to the substrate. The camera is a UEYE model 5120RE-M-GL high dynamic range camera. Dynamic range defines the ratio of the highest to lowest brightness values and is expressed in decibels (dB). For a typical camera, where the pixel value is a linear function of optical intensity, the dynamic range is 60 dB. For the UEYE camera, where the pixel value is a logarithmic function of scene brightness, the dynamic range is 120 dB. It was thought that a HDR camera would be superior for AM applications in presence of the large intensity plasma emissions that illuminate the field of view. In addition to using a HDR camera to avoid saturation, the optical path contains a 700 nm band-pass filter with a full-width half-maximum of 40 nm.

The maximum frame rate of the UEYE camera is 50 frames per second (fps) with a rolling shutter that captures one row of pixels at a time, allowing the pixels on the remaining rows to change with the scene. In contrast, most cameras use a global shutter where the image is frozen across all pixels during the readout process. This subtle point is important to consider when imaging the melt pool, as rapidly moving objects are distorted. For example, a square box moving in the field of view appears as a parallelogram. The UEYE camera uses 10 μm pixels in a 768 by 576 grid. Using a plano convex lens, the field of view is a 0.61 in by 0.46 in rectangular box centered at the laser interaction point. The resolution is approximately 0.8 mils per pixel.

A dedicated computer acquires images from the UEYE camera using a Gigabit Ethernet (GigE) interface and records the scanning speed and position as well as laser power which are provided as 0 – 10 V signals from the LENS system every 50 ms.

All experiments use Inconel 718 substrate and -120/325 MESH powder. The 6-in by 1-in ground finished substrate is 0.25 in thick and preheated to 300°C. Processing occurs in a positive-pressure, argon-filled chamber, maintained at 1 in to 3 in of water gauge pressure. Oxygen is below 20 ppm during processing. The measured Inconel powder flow rate is 6.56 grams per minute.

The analysis presented here uses data acquired in two experiments. In the first experiment, the scanning speed is set to a nominal value of 25 ipm while the laser power undergoes six step changes as indicated in the left plot in Figure 1. Similarly, in the remaining experiment, the laser power is set to a nominal value of 350 W while the scanning speed undergoes the six step changes indicated by the right plot in Figure 1. For each step, the scan position advances 0.7 in.

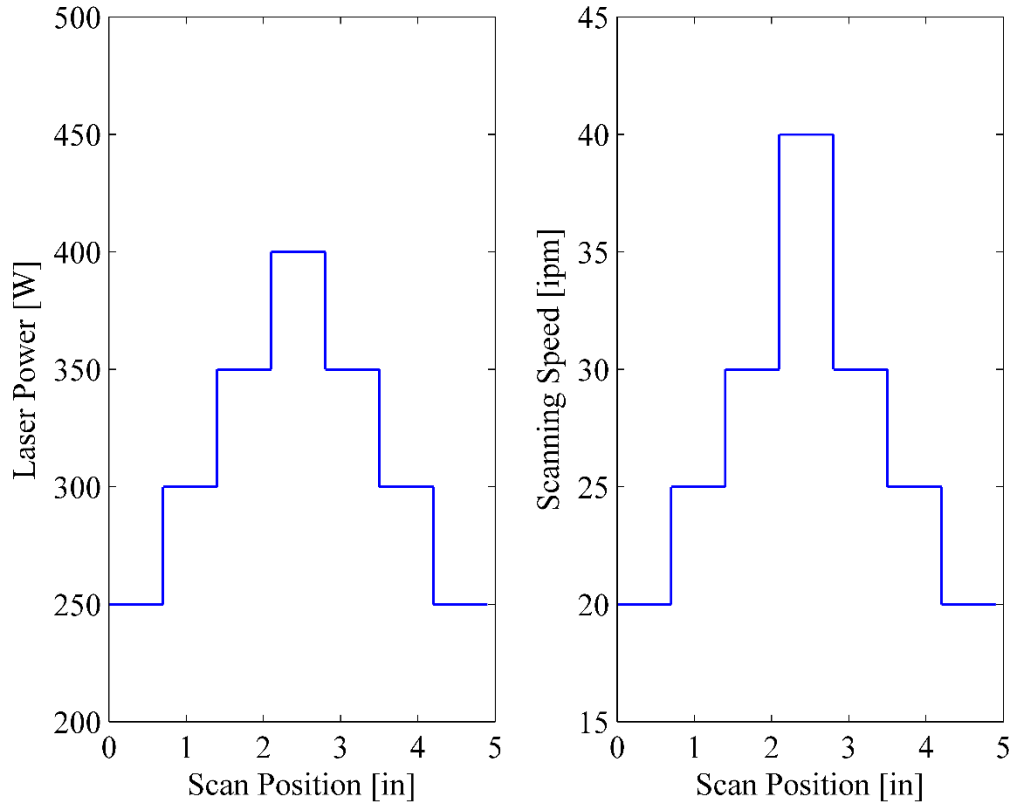


Figure 1. Variation in the manipulated variable for a fixed scanning speed of 25 ipm (left plot) and a fixed laser power of 350 W (right plot).

During each run the data acquisition system acquires an image of the melt pool every 100 ms. An estimate of melt pool width is obtained using a threshold detector to identify the boundary between the solidified metal and the melt pool. An estimate of the build height is obtained under the assumption that the brightest region in the field of view corresponds to the surface of the melt zone directly under the laser. Under this assumption, variations in the location of the brightest region in the field of view map to changes in build height.

Following the experiments, a ground truth for melt pool width and build height is obtained using an optical profilometer with a resolution on the order of nanometers. Using this device, the melt pool width and build height are determined approximately every 0.0002 in along the scan direction. As the relationship between scan position and time is independently recorded by the data acquisition system, the optical profilometer measurements may be plotted as either a function of scan position or time. For the nominal scanning speed of 25 ipm, the effective temporal sample rate of the optical profilometer measurements is approximately 2 kHz.

3. Results and Data Analysis

The melt pool width and build height derived from the camera and optical profilometer measurements are not in agreement. The camera images do not reveal a sharp boundary between the solidified metal and melt zone, making an accurate estimation of melt pool geometry difficult. The cause may be the fact that at 700 nm, the blackbody radiation from the heated substrate is of similar pixel intensity to the melt pool. In support of this argument, the rise-time of the response from laser power to build height is 20 s and 90 ms for data acquired from the camera and optical profilometer, respectively. The longer rise-time associated with the camera data is consistent with that reported by researchers who observed temperature changes in the solidified metal [3]. Another shortcoming of the camera system is that maximum frame rate of 50 fps is too slow. In general, the sample period of a control system is chosen so that at least five samples are acquired during the rise-time [7]. For the rise-times observed using the optical profilometer, the camera sample rate should be in excess of 100 fps. For these two reasons, dynamics models are identified solely from optical profilometer measurements. Furthermore, the feedback designs are not verified experimentally as accurate real-time measurements of melt pool width and build height are unavailable.

The sensitivity of a process output y in response to a change in a process input u is defined as the ratio of the percent change in the output and the percent change in the input, and is denoted as

$$S_u^y = \frac{\text{percent change in } y}{\text{percent change in } u}. \quad (1)$$

The time for a process output to raise from 10% to 90% of its final value defines the rise-time. Table 1 shows the measured rise-time and sensitivities for each output with respect to each input.

Table 1. The rise-time and sensitivity of each output with respect to each input.

Manipulated Variable	Build Height		Melt Pool Width	
	Rise Time [ms]	Sensitivity	Rise Time [ms]	Sensitivity
Laser Power	89.2	0.435	249	0.953
Scanning Speed	161	-1.26	98.7	-0.248

Using a batch least-squares estimation technique, a small-signal linear time-invariant model is estimated between each process input and output [7]. Denoting $y(k)$ as the response of the experimental system to an input $u(k)$ at the k^{th} sample instant, and $y_{LSE}(k)$ as the response of the estimated model to $u(k)$, the least squares method identifies the model that minimizes the sum of the squared errors

$$J = \sum_{k=0}^{N-1} [y(k) - y_{LSE}(k)]^2 \quad (2)$$

for N sample instants. Figures 2 through 5 show the measured response of the AM process (solid curve) and the identified model (dashed curve) as function of time for models relating scanning

speed to build height, laser power to build height, scanning speed to melt zone width, and laser power to melt pool width, respectively.

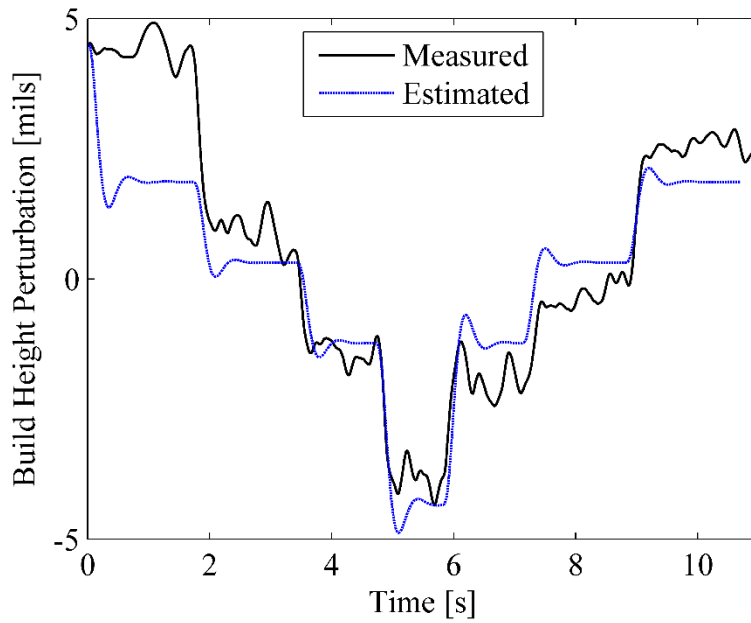


Figure 2. The response of the measured (black) and estimated (blue) build height for a nominal laser power of 350 W and the step changes in scanning speed as shown in Figure 1.

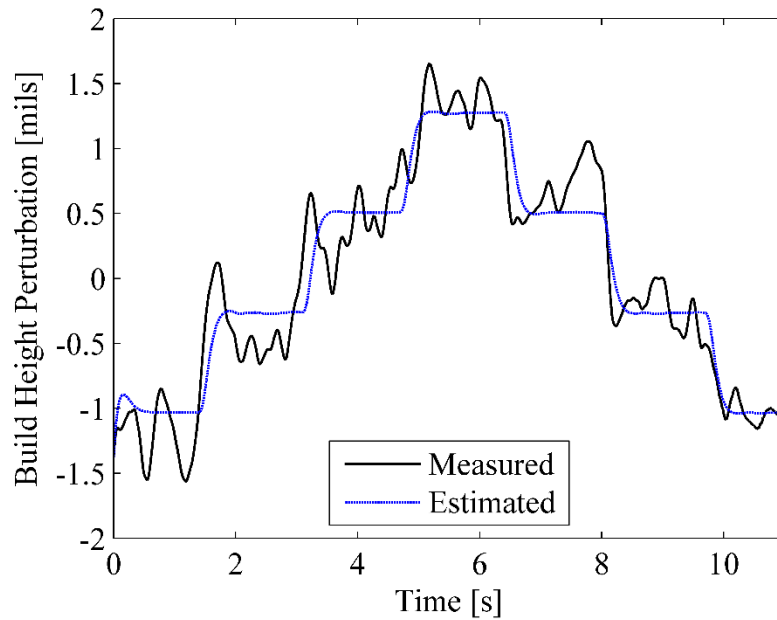


Figure 3. The response of the measured (black) and estimated (blue) build height for a nominal scanning speed of 25 ipm and the step changes in laser power as shown in Figure 1.

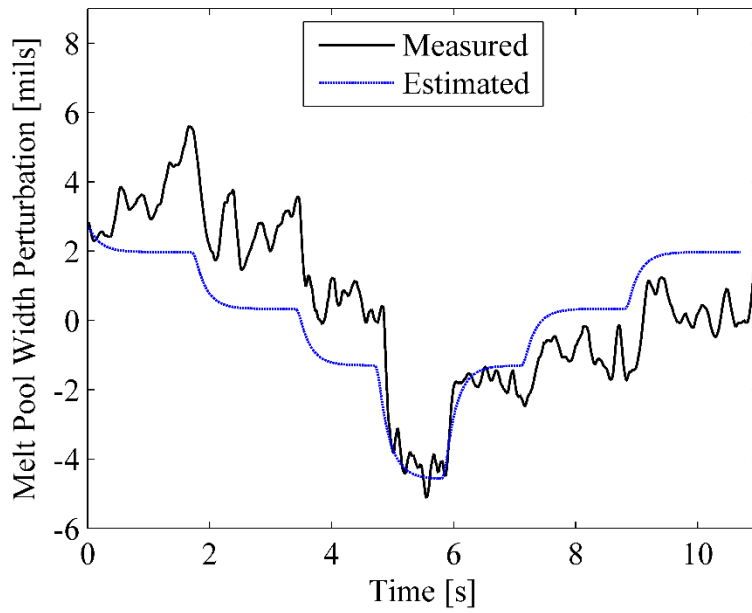


Figure 4. The response of the measured (black) and estimated (blue) melt pool width for a nominal laser power of 350W and the step changes in scanning speed as shown in Figure 1.

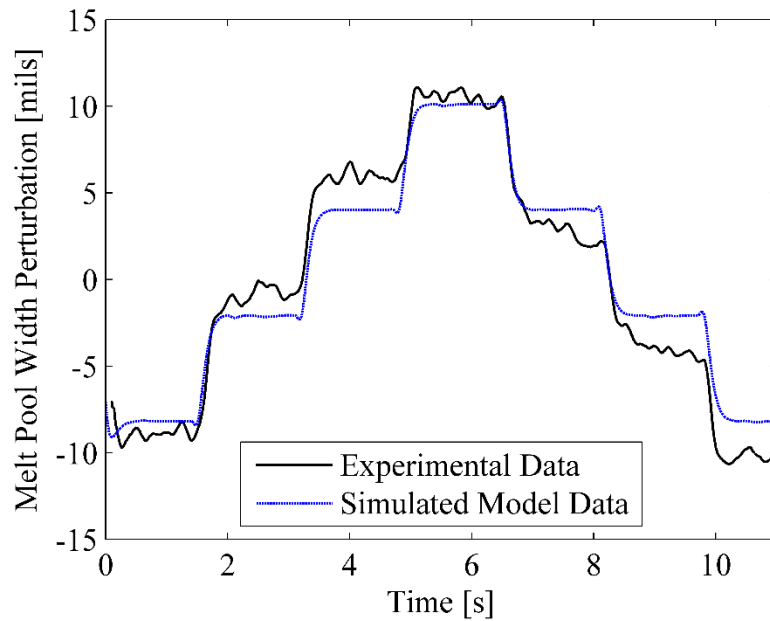


Figure 5. The response of the measured (black) and estimated (blue) melt pool width for a nominal scanning speed of 25 ipm and the step changes in laser power as shown in Figure 1.

Figures 3 and 5 show the effect of stepping laser power on build height and melt pool width, respectively. Observe that the experimental response in these variables are symmetric about 5.5 s, which is expected given the symmetry in the laser power steps shown in Figure 1. The estimated models that relate laser power to build height and melt pool width produce estimates that are in good agreement with the experimental measurements. In contrast, the experimental measurements in Figures 2 and 4 are not symmetric around 5.5 s. Based on the step changes in scanning speed in Figure 1, it is reasonable to expect that the values of build height should be the same at the beginning and end of the experiment. However, from Figure 2, the build height at the beginning and end of the experiment differ by 2 mils. Similarly, in Figure 4, the pool width at the beginning and end of the experiment also differ by 2 mils. As result, the identified models do not accurately predict the response of build height and melt pool width to scanning speed. Further studies aimed at reconciling this behavior are underway and will be reported at a later date.

The sensitivity values in Table 1 show that while both inputs affect both outputs, the sensitivities are not equal. For example, a 1% decrease in scanning speed increases the build height by 1.26%, whereas a 1% increase in laser power increases the build height by only 0.435%. The block diagram representation of the AM process model in Figure 6 indicates these relative weightings. The solid green line shows the strong coupling between scanning speed and build height, while the dashed red line shows the weak coupling between laser power and build height. The coupling between each input and output demands that the AM process be considered as a MIMO system when designing a feedback system for regulating melt pool geometry. Otherwise, regulating one output variable to a desired value may result in an undesirable steady-state value or transient response in the other variable.

As an example, Figure 6 shows one possible design strategy for regulating melt pool width and build height that uses two proportional-plus-integral (PI) controllers. Because of the weak coupling between laser power and build height, it is tempting to choose a constant laser power and design a PI controller that regulates build height by manipulating scanning speed. Similarly, because of the weak coupling between scanning speed and melt pool width, one can fix the scanning speed and design a PI controller for regulating melt pool width by manipulating laser power. Using the identified models, and assuming that the weakly coupled input is held to a constant nominal value, the PI controllers are tuned to yield a rise-time and peak-overshoot of approximately 100 ms and 5%, respectively.

Figure 7 shows the response of the closed-loop system in Figure 6 to step changes in the desired values of build height and melt pool width. In the upper (lower) subplot, the solid blue curve shows the desired build height (melt pool width) while the red curve shows the simulated build height (melt pool width), as a function of time. In the upper subplot, a 1 mil increase in build height is commanded at the 1 s time mark, and the simulated response indicates that the desired value of build height is achieved in about 1 s as the build height PI controller automatically adjusts the scanning speed. The variation in scanning speed also has a significant, and undesirable, effect on the melt zone width as shown in the lower subplot. Similarly, commanding a change in melt pool width at 4 s generates an undesirable change in build height. These undesirable changes can be avoided by taking into account the weak coupling between inputs and outputs when designing the control system.

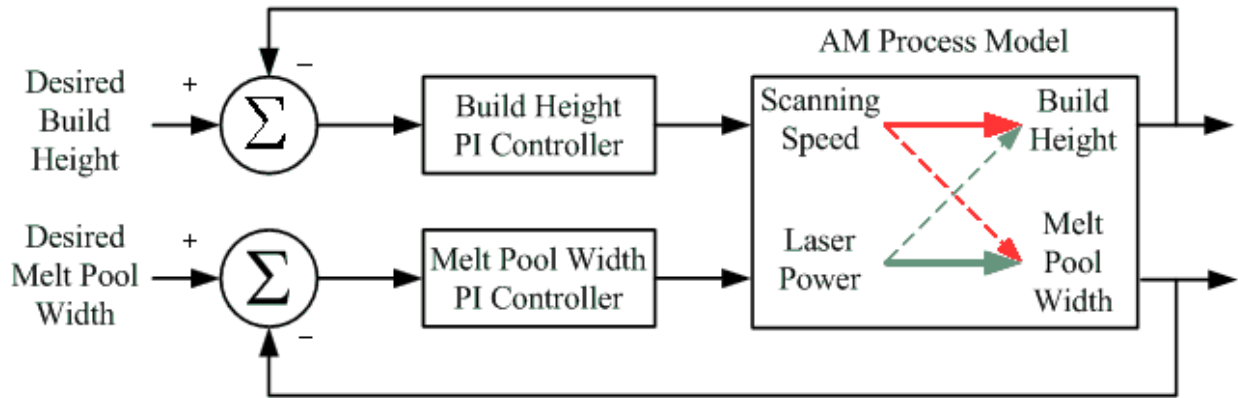


Figure 6. This candidate control design for regulating melt pool geometry yields an undesirable response because of cross-coupling between process inputs and output.

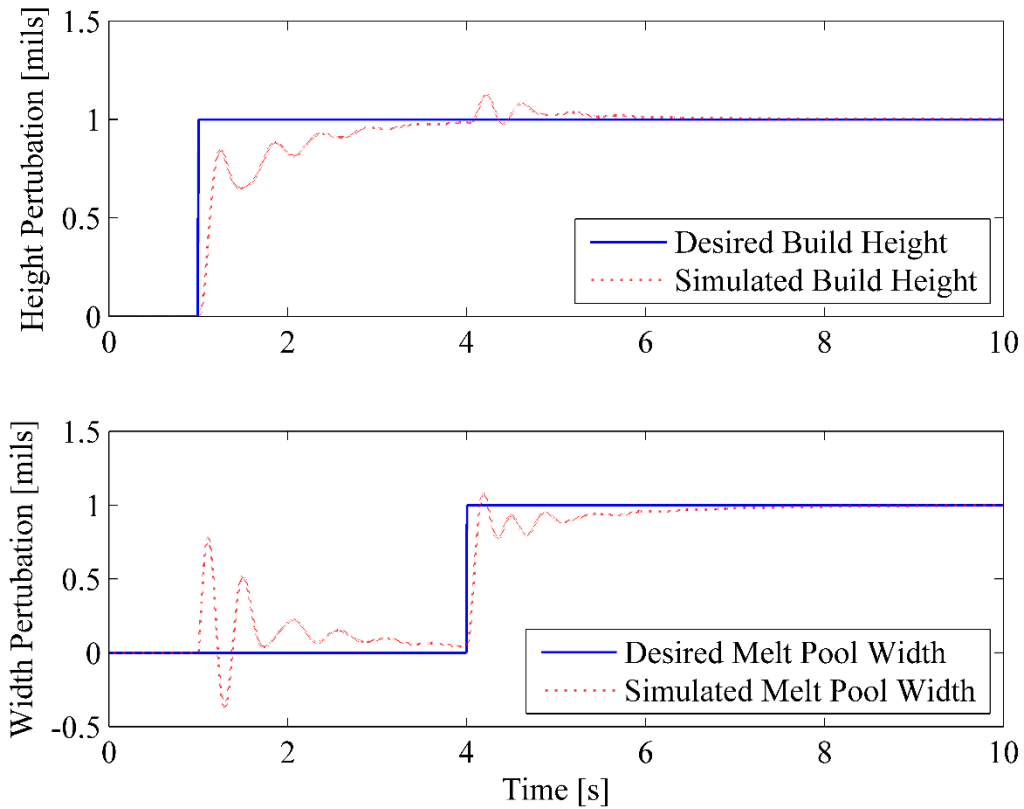


Figure 7. Simulated closed-loop response of the AM process

4. Conclusions

The results of this study motivate changes in the optical system for observing melt pool geometry, the shape of inputs used in the system identification experiments, and the strategy for designing feedback controllers that regulate geometry in AM processes. Optical emissions from the heated material, excited gases, and plasma formation make it difficult to estimate melt pool geometry parameters from acquired images. Due to strong emissions at 700 nm, it is advisable to avoid this region and acquire image at a different wavelength where the spectral emissions are smaller. This approach will most likely require an external source to illuminate the melt pool region. In addition, taking into account the time scale of fluctuations in geometry parameters, the camera system should have a frame rate of at least 100 fps and use a global shutter to minimize motion distortion.

In order to understand why the response of build height and melt pool width to changes in scanning differ from that expected, it would be useful to employ an input that momentarily perturbs an output from either side of its nominal value. Figure 8 shows one possible set of steps for achieving this goal.

Once the optical system has been modified so that real-time measurements of weld pool geometry are consistent with optical profilometer measurements, and when identified process models accurately predict the behavior of melt puddle geometry parameters with respect to changes in scanning speed, and effort will be made to design a MIMO control system that can simultaneously regulate build height and melt pool width.

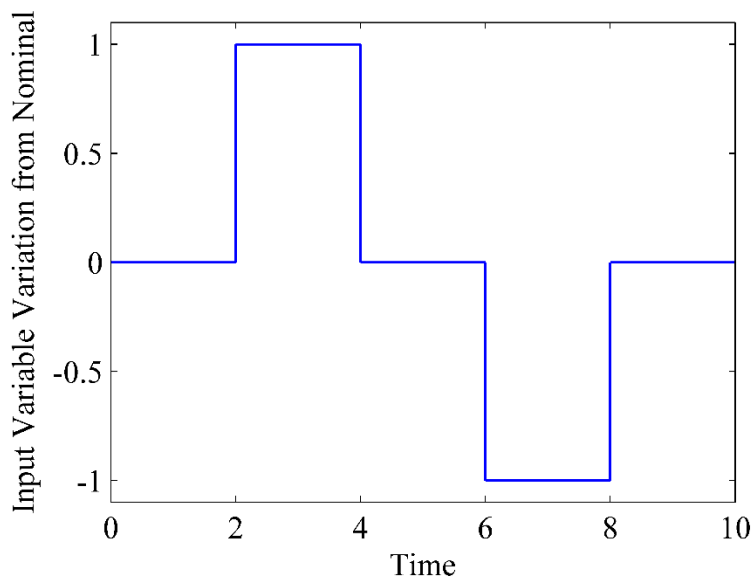


Figure 8. Alternate input waveform for system identification systems.

Acknowledgements

The authors gratefully acknowledge the contributions by Zachary Lassman, Mike Gidaro, Seth Gregor, and Chris Howland from the School of Electrical Engineering and Computer Science at the Pennsylvania State University.

This work was supported by the College of Engineering Research Initiative at The Pennsylvania State University and the Office of Naval Research, under Contract No. N00014-11-1-0668. Any opinions, findings and conclusions or recommendations expressed in this publication are those of the authors and do not necessarily reflect the views of the Office of Naval Research.

References

- [1] E. Reutzel and A. Nassar, "A survey of sensing and control systems for machine and process monitoring of directed-energy, metal-based additive manufacturing," in *Solid Freeform Fabrication Proceedings*, Austin, TX., 2014.
- [2] A. Fathi, A. Khajepour, and E. Toyserkani, "Clad height control in laser solid freeform fabrication using a feedforward PID controller," *Int. J. Adv. Manuf. Technol.*, vol. 35, no. 3-4, pp. 280-292, 2007.
- [3] L. Tang and R. Landers, "Melt Pool Temperature Control for Laser Metal Deposition Processes – Part 1," *ASME J. Manuf. Sci. Eng.*, vol. 132, no. 1, pp. 011010:1-9, 2010.
- [4] J. Hofman, B. Pathiraj, J. van Dijk, D. de Lange, and J. Meijer, "A camera based feedback control strategy for the laser cladding process," *J. Mat. Pro. Technol.*, vol. 212, no. 11, pp. 2455-2462, 2012.
- [5] D. Hu, H. Mei and R. Kovacevic, "Improving solid freeform fabrication by laser-based additive manufacturing," *Proc. Instn. Mech. Engrs.* Vol. 216, no. 11, pp. 1253-1264, 2002.
- [6] A. Heralic, A. Christiansson, M. Ottosson, and B. Lennartson, "Increased stability in laser metal wire deposition through feedback from optical measurements," *Opt. Las. Eng.*, vol. 48, no. 4, pp. 478-485, 2010.
- [7] Charles L. Phillips and H. Troy Nagel. *Digital Control System Analysis and Design*, third edition, Prentice Hall, 1995.